INTERACTION OF THE ETA-MESON WITH LIGHT NUCLEI.

by

JEAN SCHEPERS DE VILLIERS

submitted in part fulfilment of the requirements for the degree of

MASTER OF SCIENCE

in the subject

PHYSICS

at the

UNIVERSITY OF SOUTH AFRICA

SUPERVISOR: DR. RAKITYANSKI

NOVEMBER 2005

Abstract

The long-standing problem of possible formation of metastable states in collisions of the eta-meson with atomic nuclei is revisited. The two-body eta-nucleon interaction is described by a local potential, which is constructed by fitting known low-energy parameters of this interaction. The many-body eta-nucleus potential obtained within the folding model, is used to search for metastable states of the systems formed by the eta-meson with hydrogen and helium isotopes. It is found that all these systems generate strings of overlapping resonances.

Keywords:
Eta-meson, eta-nucleon interaction, eta-nucleus interaction, light nuclei, hydrogen, deuteron, triton, helium, helion (He-3), resonances, quasibound states, folding potential, density function.

DECLARATION

I declare that *Interaction of the Eta-meson with Light Nuclei* is my own work and that all sources that I have used or quoted have been indicated and acknowledged by means of references.

Signature _____ Date _____

ACKNOWLEDGEMENTS

My sincere gratitude to my supervisor **Dr. S. A. Rakityanski** for introducing me to the scattering field. My deepest appreciation goes to him for his guidance, advice and patience during this time.

I am also grateful to Dr. M. Braun for assistance in matters of computation, the contract and other administrative duties. His moral support throughout the course of this project is much appreciated.

My utmost appreciation goes to my parents, brother and other family members, both near and from afar, for giving me the moral support without which this dissertation wouldn't have seen the light of day.

Last but not least the glory goes to the Lord in heaven who gave me the strength, perserverence and courage to study the physical universe He has created.

Contents

1 Introduction **1**
1.1 Discovery and Properties of the η-meson 1
1.2 Quest for quasi-bound η-nucleus systems 3

2 Model **5**
2.1 ηN potential 5
2.2 η-nucleus potential 6
2.3 Nuclear wave functions 9
2.4 Density functions 11

3 Method for locating resonances **17**
3.1 Schrödinger equation 17
3.2 First order equations 17
3.3 Jost function and spectral points 18
3.4 Resonances 19
3.5 Complex rotation 19

4 Results **21**

5 Conclusions **31**

Bibliography **32**

Chapter 1

Introduction

1.1 Discovery and Properties of the η-meson

The η-meson was discovered in 1961 by a John Hopkins University team at Berkeley on the Bevatron accelerator [1]. This was done when physicists had already understood that many "elementary" particles known at that time, in fact, were not elementary, and tried to find out what they were made of. Theorists were looking for an adequate classification of the particles, based on the group theory, and experimentalists supplied them with necessary data. The Berkeley's discovery came at the right time since the η-meson was nicely fitted into the octet of other mesons, a group of particles with more or less similar properties, in accordance with the formal group theory classification that eventually evolved into the quark theory.

Since its discovery, extensive theoretical and experimental efforts have been devoted towards achieving a better understanding of the η-meson properties and its interaction with other particles. This was due to the special role played by the η-meson in particle physics. For example, its quark composition is such that it opens up new possibilities for investigating breakdown of the Okubo-Zweig-Iizuka (OZI) rule [2] and the charge-symmetry breaking (CSB) [3]. The latter can be attributed to quantum mixing of the quark states corresponding to the η and π^0 mesons.

Although the η–meson is four times heavier, it is in many respects similar to the π^0–meson. Both are neutral, spinless, and have almost the same lifetime, $\sim 10^{-18}$ s. The kinship between the two mesons manifests itself very clearly in their decay modes. They are the only mesons that have a high probability of pure radiative decay. The pion almost entirely (98.798 %) decays into the radiative channel $\pi^0 \to \gamma + \gamma$. For the η, the purely radiative decay is also the most probable mode [4],

$$\eta \to \begin{cases} \gamma + \gamma & (38.8\%) \\ \pi^0 + \pi^0 + \pi^0 & (31.9\%) \\ \pi^+ + \pi^- + \pi^0 & (23.6\%) \\ \pi^+ + \pi^- + \gamma & (\ 4.9\%) \\ \text{other decays} & (\ 0.8\%) \end{cases} .$$

It is believed that the π^0 and η mesons are related to each other so much that their physical quantum states are mixtures of each other,

$$|\pi^0> \ = \ |\pi'> \cos\theta - |\eta'> \sin\theta,$$

$$|\eta\ >\ =\ |\pi'>\sin\theta+|\eta'>\cos\theta,$$

where $|\pi^0>$ and $|\eta>$ are the physically observed particles while $|\pi'>$ and $|\eta'>$ are their pure isotopic states and the mixing angle is expected to be $0.01<\theta<0.02$. Moreover, this mixing is one of the reasons why charge symmetry is broken, i.e. why, for example, the proton and neutron are different (see, Refs. [5, 6, 7, 8]).

Therefore, when π^0 and η are viewed as elementary particles, they look quite similar. However in the interaction with nucleons, their difference is clearly manifested. First of all, the large difference in masses of the η ($\sim 547\,\mathrm{MeV}$) and π^0 ($\sim 135\,\mathrm{MeV}$) mesons should manifest itself in the meson-nucleon dynamics. This is indeed the case at low energies. For example, the S_{11}-resonance $N^*(1535)$ is formed in both $\pi^0 N$ and ηN collisions, but at different energies,

$$\begin{aligned} E^{res}_{\pi N}(S_{11}) &= 1535\ \mathrm{MeV}\ - m_N - m_\pi\ \approx\ 458\ \mathrm{MeV}\ , \\ E^{res}_{\eta N}(S_{11}) &= 1535\ \mathrm{MeV}\ - m_N - m_\eta\ \approx\ 49\ \mathrm{MeV}\ . \end{aligned}$$

As is seen, due to the large mass of the η-meson this resonance is very close to the ηN-threshold. Furthermore it is very broad, with $\Gamma\approx 150\,\mathrm{MeV}$, covering the whole low energy region of the ηN interaction. As a result the interaction of nucleons with η-mesons in this region, where the S-wave interaction dominates, is much stronger than with pions.

Another consequence of the S_{11} dominance is that the interaction of the η-meson with a nucleon can be considered as a series of formations and decays of this resonance as shown in Fig. 1.1. Independently of the formation channel, the intermediate $N^*(1535)$-resonance decays with almost equal probabilities into the ηN and πN channels. This means that in the energy region covered by the S_{11}-resonance, the ηN and πN interactions should be treated as a coupled channel problem. When such an analysis was performed, it was found that the near-threshold ηN interaction is attractive [9]. This is very important feature of the ηN interaction since it raises the question as to whether this attraction is strong enough to bind the η-meson inside a nucleus.

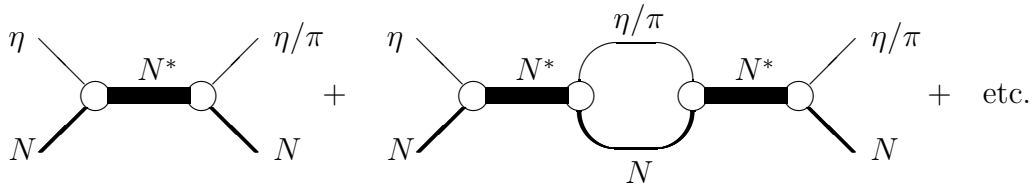

Figure 1.1: Schematic representation of the resonant two-channel scattering $\eta N\to N^*\to\eta N$ and $\eta N\to N^*\to\pi N$. The notation η/π means η or π.

Since η-mesons decay very fast, it is impossible to produce beams of them and therefore they can only be observed in final states of certain nuclear reactions. This makes investigation of η-meson dynamics quite complicated. Therefore if an η-meson could be sustained inside a nucleus for some time, it would expose itself

for a relatively long period in a series of successive interactions with nucleons, i.e., inside the nucleus it would undergo a series of absorptions and emissions through formation and decay of the $N^*(1535)$-resonance as depicted in Fig. 1.2.

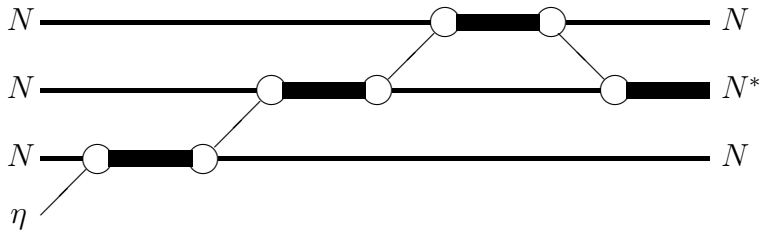

Figure 1.2: Schematic representation of the resonant η-nucleus scattering.

In such a series, after each decay of the S_{11}-resonance the η-meson is generated anew. Therefore the lifetime of an η-mesic nucleus would not be limited by the lifetime of the meson itself. However, such an η-nucleus complex cannot be stable, since eventually the $N^*(1535)$-resonance will produce a pion with huge kinetic energy of $\sim 400\,\mathrm{MeV}$ (thanks to its small mass), which will enable it to escape. It is therefore clear that if an η-meson is bound inside a nucleus, it can only be in a quasi-bound (metastable) state with a nonzero width.

Such a possibility looked very exciting and thus a search for metastable η-nucleus complexes started.

1.2 Quest for quasi-bound η-nucleus systems

First estimation obtained in the framework of the optical potential theory [10], put a lower bound on the number A of the nucleons that could be sufficient to bind the η-meson, namely, $A \geq 12$. Thereafter, other theoretical investigations were devoted to this problem [11]. All of them predicted η-nucleus bound states obeying the same constraint $A \geq 12$. However, the first experimental attempt to find η-nuclear bound states with lithium, carbon, oxygen, and aluminum produced negative results [12]. The conclusion of this experimental work did not discourage theoreticians in examining the possibility of the η-nucleus binding.

The relatively large scattering lengths obtained for η^3He and η^4He systems [13] cast some doubt on the $A \geq 12$ constraint. Moreover, in the measurements of the η-production on nuclei by γ-quanta and other particles, it was found that the cross-section strongly depends on the energy and is practically isotropic [14, 15], which can be explained by formation of either a bound or a resonant η-nucleus state. Indeed, if the η-meson is trapped by a nucleus, their bound or resonant state can be formed at a specific energy, any shift from which must lead to a significant decrease of the cross-section, which means strong energy dependence. And after being captured, the meson forgets the direction of incidence, which means that the decay of such state must be isotropic.

The first microscopic few-body calculations of the η-meson scattering from d, t, ^{3}He, and ^{4}He nuclei were presented in Ref's. [16, 17]. By locating the S-matrix poles

in the complex momentum plane, it was found that with the uncertainties of the parameters of the η-nucleon potential, even the existence of η-deuteron quasi-bound state could not be excluded. This work boosted the activity around possible bound states of the η with light nuclei. Many theoretical papers claimed the discovery of such states on the basis of simplified calculations [18]. New experimental work also gave strong evidence supporting the existence of near-threshold bound or resonance states of the η with ^{11}B, ^{11}C, ^{4}He, and even the deuteron [19]. Such evidence, however, remains inconclusive because of being based on indirect observations of the enhancement of the final state interaction between the η and the nucleus, which takes place at low positive energies. The quasi-bound states, if any, are also not far from the zero energy, but on the negative side. In this dissertation, therefore, we explore the near-threshold positive energies.

Being of interest by itself, the existence of η-nuclei would also shed new light on various fundamental problems of particle physics. This is why so much effort has been devoted to understanding the η-nucleus dynamics and searching for long-lived η-nucleus complexes. Our work is another step in this direction.

In contrast to all previous calculations, which were based on a one-term separable ηN interaction, we construct a local ηN potential. This enables us to use the very powerful Jost function method to look for metastable states formed by the η-meson with hydrogen and helium isotopes. We found that all these systems generate strings of overlapping resonances.

The dissertation is structured as follows. Chapter 2 describes the model assumptions used in our calculations, such as the ηN-potential, η-nucleus potential and nuclear wave functions. In Chapter 3 methods, e.g. Complex Rotation, for solving the Schrödinger equation and finding the spectral points with the Jost function are outlined. The resonances are given in Chapter 4. The conclusions then follows in the last chapter.

Chapter 2

Model

2.1 ηN potential

As was already said in the Introduction, when the ηN interaction is considered, it is necessary to take into account the πN channel, i.e. the transitions

$$\eta N \to \pi N \to \begin{cases} \eta N \\ \pi N \end{cases} \to \cdots \ .$$

The fact that the pion has a much smaller mass, offers a way to simplify the treatment of this two-channel problem. Indeed, the transition $\eta N \to \pi N$ is accompanied by the release of $\sim 400\,\mathrm{MeV}$ of kinetic energy. As a result, the pion and nucleon move very fast relative each other and therefore have a very short time to interact. This means that the probability of coming back to the initial channel via the reverse transition $\pi N \to \eta N$ is negligible. Therefore, we can safely assume that if the η happens to undergo the transformation into the pion, it never comes back and is lost forever.

In quantum mechanics, such disappearances of particles are formally described by adding an imaginary part to the potential [20]. Thus, instead of considering the ηN and πN systems as a two-channel problem, we can assume that the ηN intercation is decribed by an effective one-channel complex potential.

Since the η beams are not available and direct scattering experiments with them are not possible, the quantitative data that can be used to construct the ηN potential are very scarce. The only known quantities are the position $E(S_{11})$ of the pole of the ηN scattering amplitude, corresponding to the S_{11} resonance, and the scattering length $a_{\eta N}$, i.e. the value of the amplitude at zero collision energy. Even this scarce information [21],

$$\begin{aligned} E(S_{11}) &\approx (49 - i75)\,\mathrm{MeV}\ , \\ 0.2\,\mathrm{fm} \le \mathrm{Re}\, a_{\eta N} &\le 1.0\,\mathrm{fm}\ , \\ 0.2\,\mathrm{fm} \le \mathrm{Im}\, a_{\eta N} &\le 0.4\,\mathrm{fm}\ , \end{aligned}$$

is not very accurate. In all previous publications, the ηN potential was constructed in the momentum space and in the separable form, i.e. was non-local. Here we present the first attempt to describe the ηN interaction by a local potential in configuration space. Although it is more difficult to construct such a potential, it

opens up new possibilities for exploring the resonance spectra of η-nucleus systems. This is because with a local potential, we can use the Jost function method (see Ref.[22, 23]) for locating resonances.

As a starting point, we chose the following functional form for the ηN potential

$$V_{\eta N}(r) = a_1 e^{-b_1(r_1-r)^2} - a_2 e^{-b_2 r^2} - i a_3 e^{-b_3 r^2} \ , \tag{2.1}$$

where the first term is a barrier responsible for the S_{11} resonance, the second term gives a short-range attraction, and the last one is the absorptive part that takes care of all inelastic processes.

Then, using a fitting procedure within the Jost function method, we found the set of parameters shown in Table 2.1, which give

parameter	value
r_1	1.95616478619031975 fm
a_1	57.5826586837329657 MeV
a_2	26.8157044304329091 MeV
a_3	0.603932024464326478 MeV
b_1	$0.0715471865601824408\,\mathrm{fm}^{-2}$
b_2	$0.0271505486074286040\,\mathrm{fm}^{-2}$
b_3	$0.0338015704618582769\,\mathrm{fm}^{-2}$

Table 2.1: Parameters of the ηN potential (2.1).

$$E(S_{11}) = (48.57 - i75.05)\,\mathrm{MeV}$$

and

$$a_{\eta N} = (0.75 + i0.27)\,\mathrm{fm} \ .$$

These figures were obtained via the procedure of minimization. These figures are intermediate computer results which are used in further calculations. This is why there is so many decimal places.

Within the above uncertainty interval, this value for the scattering length is considered as the most probable one since different analyses give the results concentrated around it. The potential corresponding to these parameters is shown in Figs. 2.1 and 2.2.

The two-body ηN potential is the main building block of our model. Using it, we construct the effective potentials that describe interaction of the η meson with light nuclei. This is done in the next section in the framework of the folding model.

2.2 η-nucleus potential

When the η meson approaches a nucleus it feels the forces generated by all the nucleons which the nucleus consists of. These forces depend on distances between the

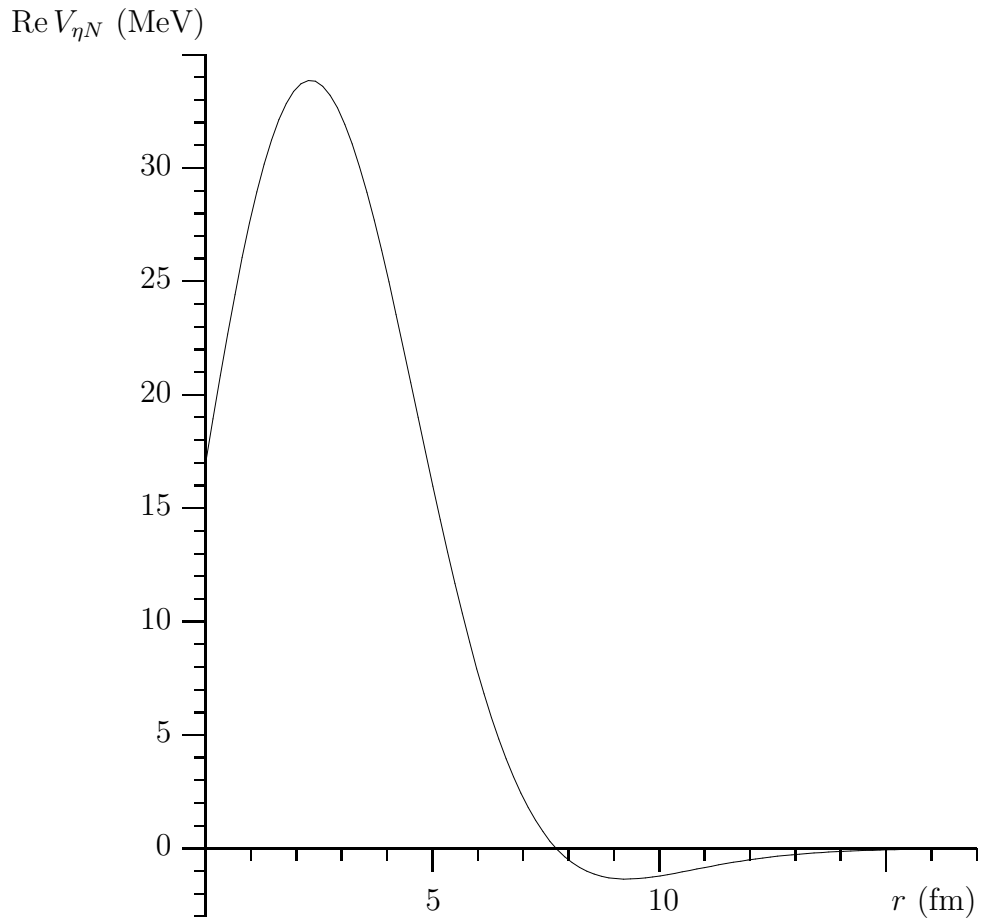

Figure 2.1: Real part of the ηN potential (2.1) as a function of the distance between the η and N.

meson and each individual nucleon. These distances are determined by the distance r between the meson and the nucleus centre of mass as well as by the positions $\vec{r}_i$ of the nucleons inside the nucleus (see Fig. 2.3). The meson moves relative to the nucleus and the nucleons constantly move inside the nucleus. At every instance the total η-nucleus potential energy is a sum of individual ηN_i potentials depending on their individual positions.

The η-nucleus potential is therefore a complicated function of time. This however can be significantly simplified if we take into account the fact that at low collision energies (which we are considering) the nucleons move inside the nucleus much faster than the meson approaches or moves away. This means that while the meson makes a small move (small change of r), the nucleons have enough time to go through all possible spatial configurations $\{\vec{r}_1, \vec{r}_2, \ldots \vec{r}_A\}$. The probabilities of different configurations are determined by the nuclear wave function $\psi_A(\vec{r}_1, \vec{r}_2, \ldots \vec{r}_A)$.

As a result of fast movement of the nucleons, the meson feels the collective force which is the statistical average over all possible configurations. In other words,

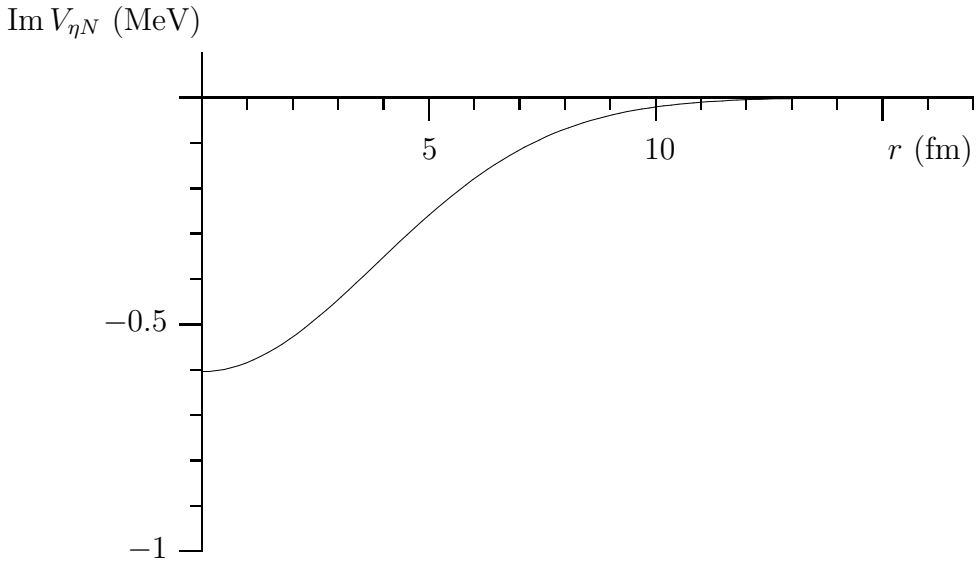

Figure 2.2: Imaginary part of the ηN potential (2.1) as a function of the distance between the η and N.

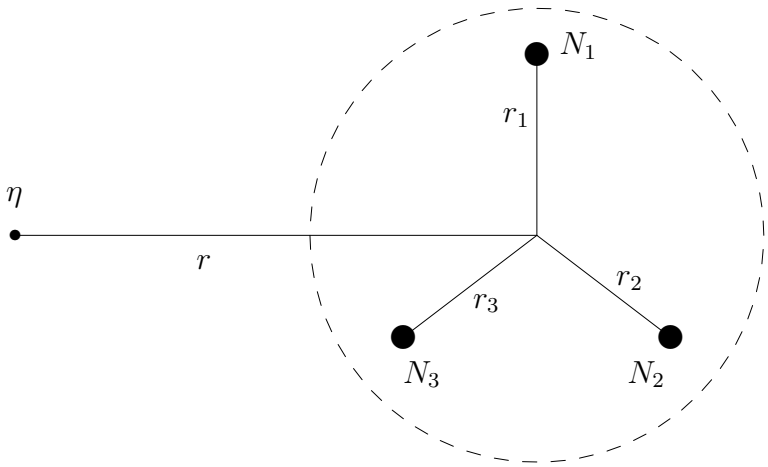

Figure 2.3: Schematic representation of an η-nucleus system.

it moves in the potential field described by the effective potential

$$V_{\eta A}(r) = \int \sum_{i=1}^{A} V_i(|\vec{r} + \vec{r}_i|)\, |\psi_A(\vec{r}_1, \vec{r}_2, \ldots \vec{r}_A)|^2 \, \mathrm{d}\vec{r}_1 \mathrm{d}\vec{r}_2 \ldots \mathrm{d}\vec{r}_A \ , \qquad (2.2)$$

which is called *folding potential* [24].

It should be emphasized that the use of the potential (2.2) to describe the η-nucleus interaction is an approximation, which is valid for low collision energies.

2.3 Nuclear wave functions

In the present dissertation, we analyze the interaction of the η meson with hydrogen and helium isotopes. Strictly speaking, the corresponding wave functions needed for constructing the folding potentials (2.2), should be obtained by solving the rigorous few-body equations with realistic NN forces. This however would be a separate extremely difficult task. Furthemore, the accuracy of such wave functions would be far beyond the accuracy of the ηN potential itself. The current knowledge of the ηN interaction is rather limited. This means that in any case we are only able to estimate rather than exactly locate possible η-nucleus resonances. For this purpose, it is sufficient to use approximate wave functions of the nuclei.

In the system of reference tied to the nucleus centre of mass, only $(A-1)$ of the A nucleon coordinates $\vec{r}_i$ shown in Fig. 2.3 are independent. Indeed, the fact that the origin coincides with the centre of mass means that

$$\vec{r}_1 + \vec{r}_2 + \ldots + \vec{r}_A = 0 \ .$$

This is why it is more convenient to describe the configuration of the nucleons using the so-called Jacobi vectors shown in Fig. 2.4.

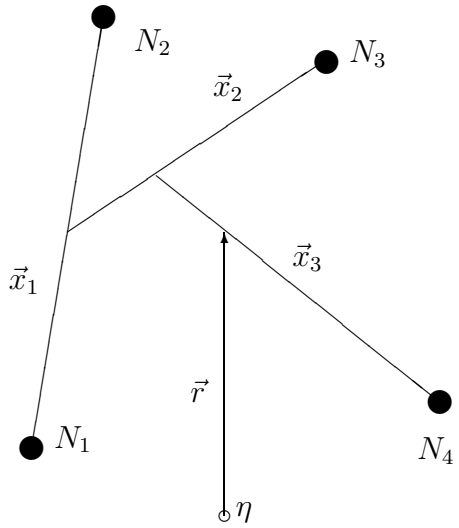

Figure 2.4: Jacobi vectors determining the spatial configuration of an η-nucleus system.

Vector $\vec{x_1}$ originates on the nucleon N_1 while $\vec{x_2}$, $\vec{x_3}$, etc. are drawn from the centre of mass of the smaller subsystem towards the additional nucleon. Vector $\vec{r}$ points to the centre of mass of the whole nucleus.

For the nuclei considered in this dissertation, namely, deuteron (d), triton (t), ^{3}He (τ), and ^{4}He (α), we use the following approximations (taken from Ref. [16])

$$\psi_d(\vec{x_1}) = \frac{K_d}{\sqrt{4\pi}} \exp\left(-k_d \frac{1}{2} x_1^2\right) \ , \tag{2.3}$$

$$\psi_{t,\tau}(\vec{x_1}, \vec{x_2}) = \frac{K_{t,\tau}}{4\pi} \exp\left[-k_{t,\tau}\left(\frac{x_1^2}{2} + \frac{2x_2^2}{3}\right)\right] \ , \tag{2.4}$$

$$\psi_\alpha(\vec{x_1},\vec{x_2},\vec{x_3}) \;=\; \frac{K_\alpha}{(4\pi)^{3/2}}\exp\left[-k_\alpha\left(\frac{x_1^2}{2}+\frac{2x_2^2}{3}+\frac{3x_3^2}{4}\right)\right]\;. \tag{2.5}$$

The wave functions of the t and τ have the same functional form and differ from each other only through the constants K_s and k_s for $s = t, \tau$.

The dependence on the Jacobi coordinates in the wave functions (2.3- 2.5) is chosen in such a way that they exponentially attenuate at large distances (as it must be for any bound state wave function) and are invariant under all possible nucleon permutations. The last requirement comes from the Pauli principle. Indeed, since nucleons are fermions, their total wave function consisting of the spatial and the spin-isospin parts, must be antisymmetric under the permutations. For the S-wave ground state, the spin-isospin part is antisymmetric, which means that the spatial part is symmetric.

The constants K_s and k_s for $s = d, t, \tau, \alpha$ are determined uniquely when two integrals, one for normalization and one for the root mean square (RMS) radius, are calculated for a system s.

In evaluating these volume integrals, a situation always arises when the folowing standard integrals [25] have to be calculated

$$\int_0^\infty dx x^2\exp(-ax^2) = \frac{1}{4a}\sqrt{\frac{\pi}{a}}\;, \tag{2.6}$$

and

$$\int_0^\infty dx x^4\exp(-ax^2) = \frac{3}{8a^2}\sqrt{\frac{\pi}{a}}\;. \tag{2.7}$$

The normalization condition

$$\int|\psi(\vec{x}_1,\vec{x}_2,\ldots,\vec{x}_{A-1})|^2 d\vec{x}_1 d\vec{x}_2\ldots d\vec{x}_{A-1} = 1$$

specifies K_s in terms of k_s. In which case, for $s = d, t, \tau, \alpha$ we obtain, respectively,

$$1 = \int|\psi_d(\vec{x}_1)|^2 d\vec{x}_1 \qquad\rightarrow\qquad K_d = \left(4k_d^{3/2}/\sqrt{\pi}\right)^{1/2}\;, \tag{2.8}$$

$$1 = \int|\psi_{t,\tau}(\vec{x}_1,\vec{x}_2)|^2 d\vec{x}_1 d\vec{x}_2 \qquad\rightarrow\qquad K_{t,\tau} = \left[4/\sqrt{\pi}\right]\sqrt{(4/3)^{3/2}\,k_{t,\tau}^3}\;, \tag{2.9}$$

$$1 = \int|\psi_\alpha(\vec{x}_1,\vec{x}_2,\vec{x}_3)|^2 d\vec{x}_1 d\vec{x}_2 d\vec{x}_3 \qquad\rightarrow\qquad K_\alpha = \sqrt{\left(\sqrt{32\,k_\alpha^3/\pi}\right)^3}\;. \tag{2.10}$$

When calculating the RMS-radii of the nuclei, we now can replace the normalization constants K_s with the expressions (2.8-2.10) and thus will have only one unknown parameter, namely, k_s for each nucleus. The integration for $s = d, t, \tau, \alpha$ gives

$$< r_d^2 >= \int d\vec{x}_1|\psi_d(\vec{x}_1)|^2\left(\frac{x_1}{2}\right)^2 \;=\; \frac{3}{8k_d}\;, \tag{2.11}$$

$$< r_{t,\tau}^2 >= \int d\vec{x}_1 d\vec{x}_2|\psi_{t,\tau}(\vec{x}_1,\vec{x}_2)|^2\left(\frac{2x_2}{3}\right)^2 \;=\; \frac{1}{2k_{t,\tau}}\;, \tag{2.12}$$

$$< r_\alpha^2 >= \int d\vec{x}_1 d\vec{x}_2 d\vec{x}_3|\psi_\alpha(\vec{x}_1,\vec{x}_2,\vec{x}_2)|^2\left(\frac{3x_3}{4}\right)^2 \;=\; \frac{9}{16k_\alpha}\;. \tag{2.13}$$

With Eqs. (2.11-2.13), the parameters k_s can be fixed using known values of the RMS-radii (see, for example Ref. [16]),

$$\sqrt{< r_d^2 >} = 1.956\,\text{fm} \ ,$$

$$\sqrt{< r_t^2 >} = 1.755\,\text{fm} \ ,$$

$$\sqrt{< r_\tau^2 >} = 1.959\,\text{fm} \ ,$$

$$\sqrt{< r_\alpha^2 >} = 1.671\,\text{fm} \ .$$

When k_s are found, the normalization constants can be calculated using Eqs. (2.8-2.10). Thus, both K_s and k_s are determined and therefore the wave functions (2.3-2.5) are completely defined.

2.4 Density functions

Nucleons are identical particles. This fact significantly simplifies calculation of the folding potential (2.2). Indeed, the wave function is symmetric and therefore it is not necessary to make a sum in (2.2) over all nucleons. It is enough to take any one of them and multiply the result by A, because their contributions are the same. Therefore

$$V_{\eta A}(r) = A \int V_i(|\vec{r} + \vec{r}_i|) \left|\psi_A(\vec{r}_1, \vec{r}_2, \ldots \vec{r}_A)\right|^2 \mathrm{d}\vec{r}_1 \mathrm{d}\vec{r}_2 \ldots \mathrm{d}\vec{r}_A \ , \tag{2.14}$$

where i is any one of the nucleon numbers. In the above equation, we can perform the integration of the wave function independently of the potential, over all nucleon coordinates except the $\vec{r}_i$. For simplicity, let $i = 1$, then

$$V_{\eta A}(r) = \int V_1(|\vec{r} + \vec{r}_1|)\rho(\vec{r}_1)\mathrm{d}\vec{r}_1 \ , \tag{2.15}$$

where

$$\rho(\vec{r}_1) = A \int \left|\psi_A(\vec{r}_1, \vec{r}_2, \ldots \vec{r}_A)\right|^2 \mathrm{d}\vec{r}_2 \mathrm{d}\vec{r}_3 \ldots \mathrm{d}\vec{r}_A \tag{2.16}$$

is the density function. It determines the distribution of the matter inside the nucleus. Since it does not matter which nucleon to choose in Eq. (2.15), it can be rewritten in a more symmetrical form

$$V_{\eta A}(r) = \int V_{\eta N}(|\vec{r} + \vec{r'}|)\rho(\vec{r'})\mathrm{d}\vec{r'} \ . \tag{2.17}$$

The choice of the functional dependence of the wave functions (2.3-2.5) is very convenient for analytical calculation of the density functions. The simplification comes from the fact that each variable in the wave functions can be separated in an exponential factor. The exponential that is not integrated, provides the density Gaussian form while the others produce constant coefficients to this Gaussian function. After

the integration, we obtain the following density functions:

$$\rho_d(\vec{r}) = 2\left(\sqrt{\frac{k_d}{\pi}}\right)^3 \exp\left[-4k_d r^2\right] , \tag{2.18}$$

$$\rho_{t,\tau}(\vec{r}) = \frac{8}{\sqrt{3}}\left(\sqrt{\frac{k_{t,\tau}}{\pi}}\right)^3 \exp\left[-3k_{t,\tau} r^2\right] , \tag{2.19}$$

$$\rho_\alpha(\vec{r}) = \sqrt{2}\left(\sqrt{\frac{3k_\alpha}{\pi}}\right)^3 \exp\left[-\frac{8}{3}k_\alpha r^2\right] . \tag{2.20}$$

As is seen, all these functions have the same Gaussian form

$$\rho_s(\vec{r}) = C_s \exp\left(-c_s r^2\right) , \tag{2.21}$$

where

$$C_d = 2\left(\sqrt{\frac{k_d}{\pi}}\right)^3 = \frac{1}{4}\left(\sqrt{\frac{c_d}{\pi}}\right)^3 ,$$

$$c_d = 4k_d = \frac{3}{2 < r_d^2 >} , \qquad k_d = \frac{3}{8 < r_d^2 >} ,$$

$$C_{t,\tau} = \frac{8}{\sqrt{3}}\left(\sqrt{\frac{k_{t,\tau}}{\pi}}\right)^3 = \frac{8}{9}\left(\sqrt{\frac{c_{t,\tau}}{\pi}}\right)^3 ,$$

$$c_{t,\tau} = 3k_{t,\tau} = \frac{3}{2 < r_{t,\tau}^2 >} , \qquad k_{t,\tau} = \frac{1}{2 < r_{t,\tau}^2 >} ,$$

$$C_\alpha = (\sqrt{3})^3\sqrt{2}\left(\sqrt{\frac{k_\alpha}{\pi}}\right)^3 = \frac{27}{16}\left(\sqrt{\frac{c_\alpha}{\pi}}\right)^3 ,$$

$$c_\alpha = \frac{8k_\alpha}{3} = \frac{3}{2 < r_\alpha^2 >} , \qquad k_\alpha = \frac{9}{16 < r_\alpha^2 >} .$$

These density functions are shown in Figs. 2.5 and 2.6. On the first of them, vertical axis is linear while the other plot shows the same densities in the logarithmic scale. The *log* scale highlights the density spread better.

With these density functions, the η-nucleus folding potential (2.2) was calculated for each of the isotopes, $s = d, t, \tau, \alpha$. The integration was done in spherical polar coordinates,

$$V_{\eta A}(r) = 2\pi \int_0^\pi \int_0^\infty \rho_s(r') V_{\eta N}\left(\sqrt{r^2 - 2rr'\cos\theta + r'^2}\right) r'^2 dr' \sin\theta d\theta , \tag{2.22}$$

with the positive z-axis aligned so that the η-meson approaches the nucleus along this axis. These potentials are shown in Figs. 2.7 and 2.8.

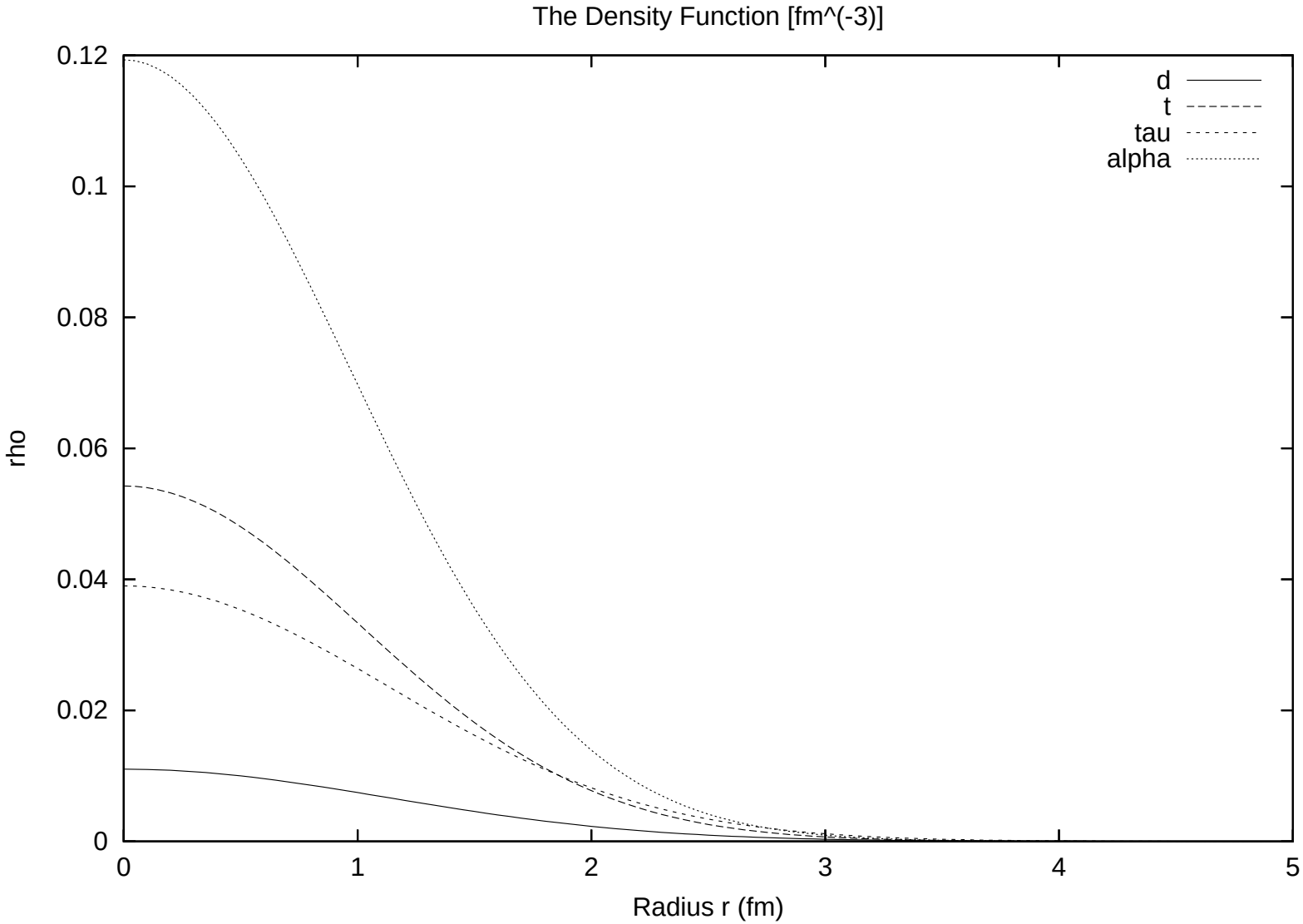

Figure 2.5: Density functions for the hydrogen and helium isotopes.

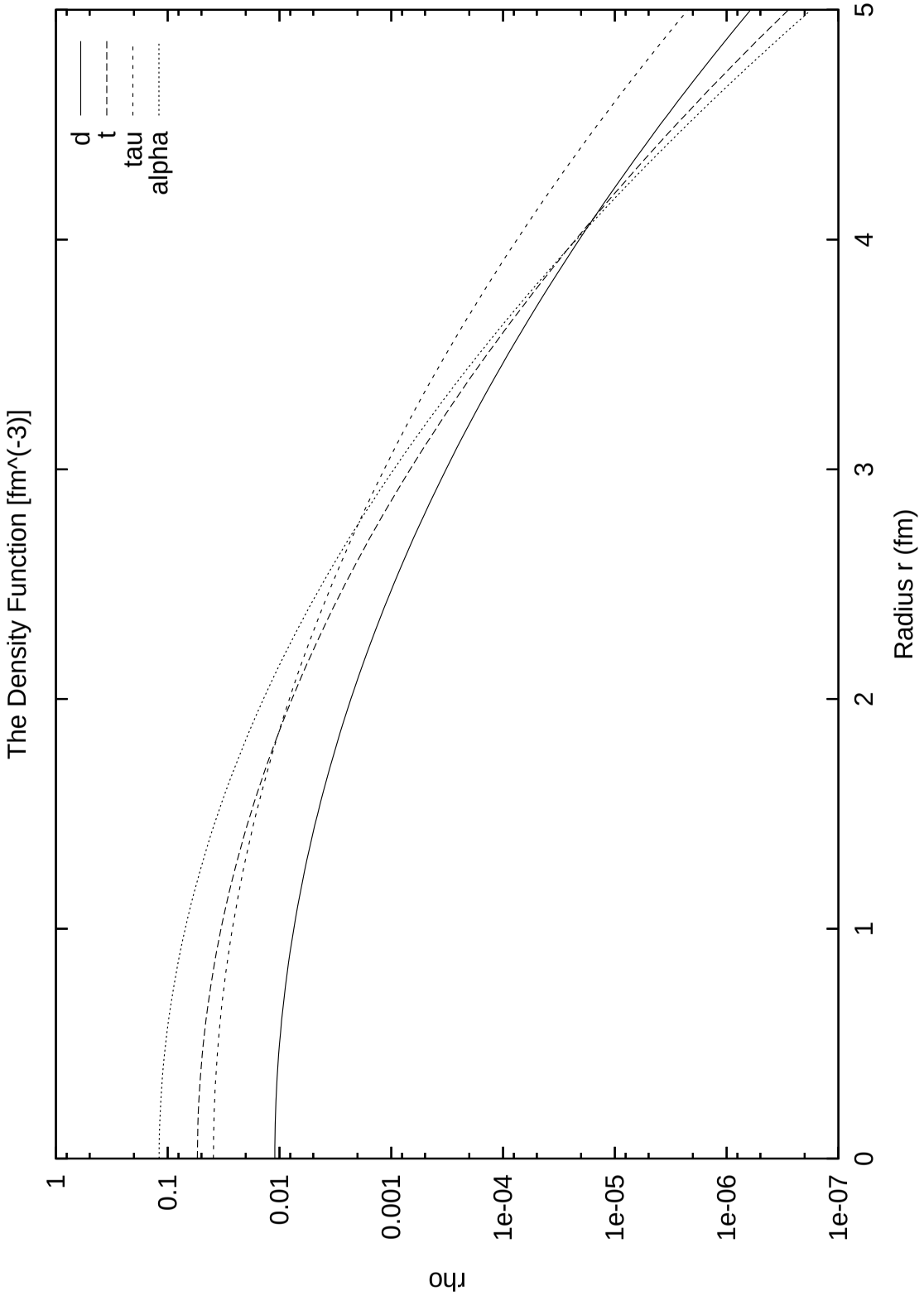

Figure 2.6: Density functions in the logarithmic scale for the hydrogen and helium isotopes.

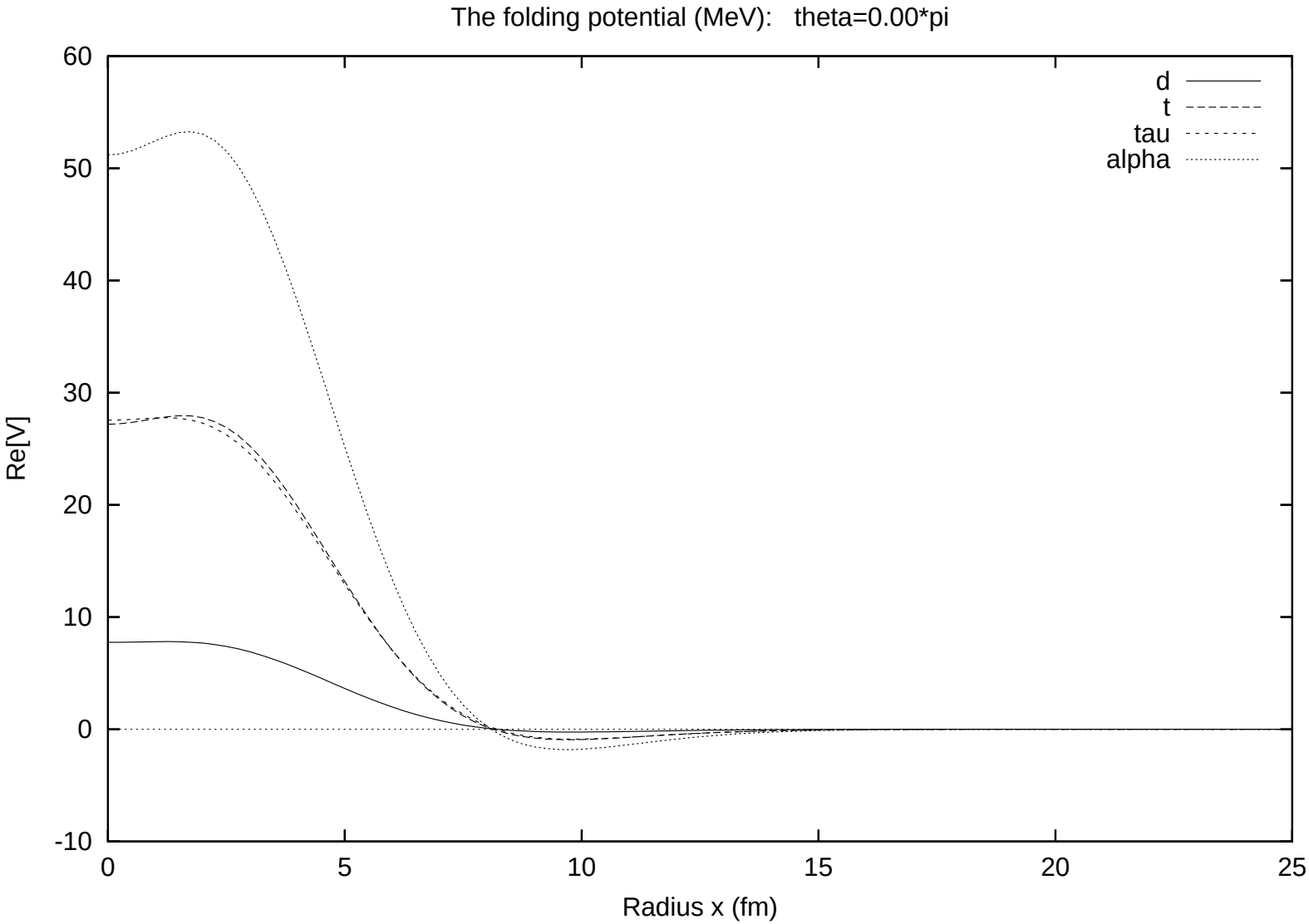

Figure 2.7: Real part of the folding η-nucleus potential for four isotopes.

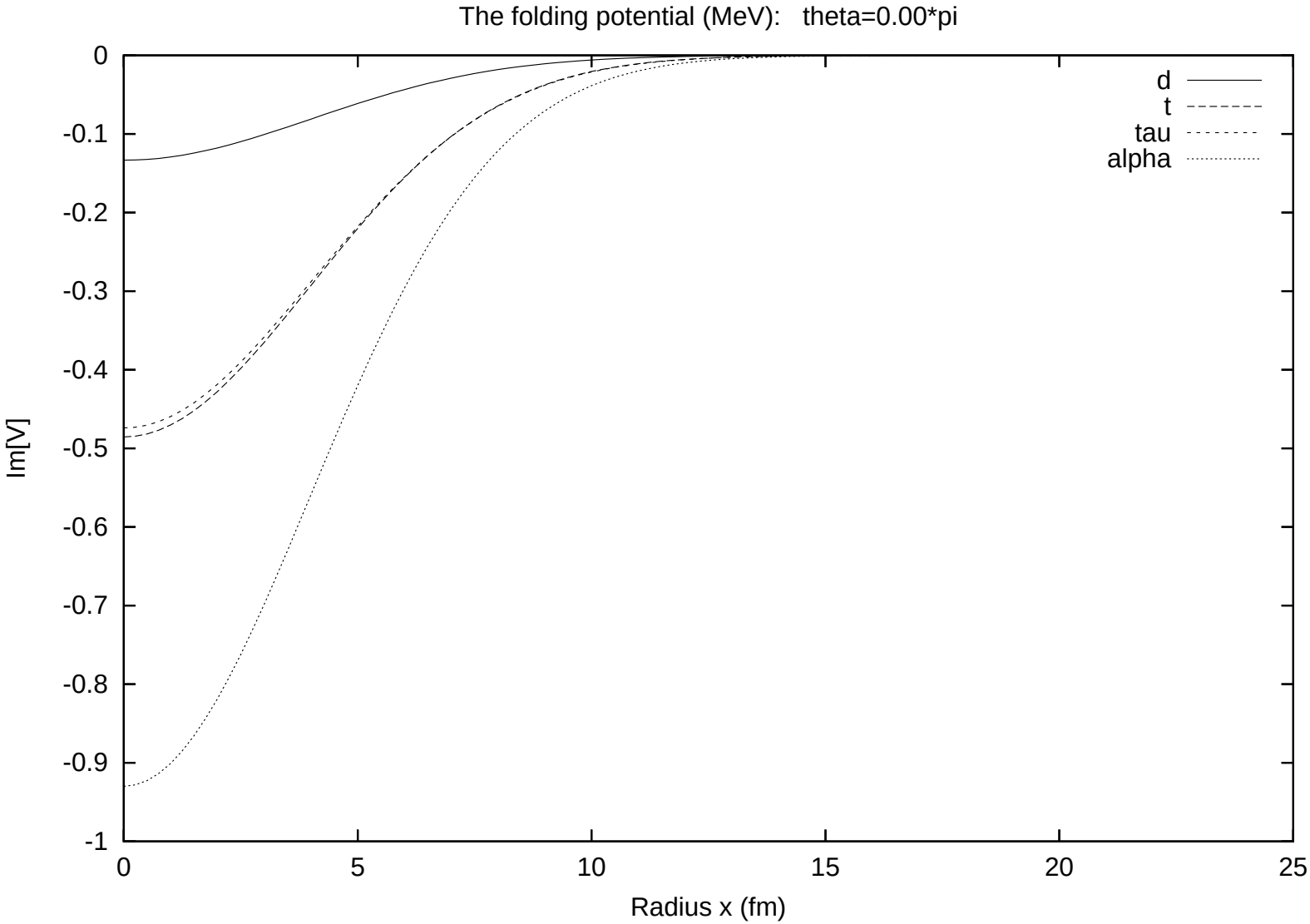

Figure 2.8: Imaginary part of the folding η-nucleus potential for four isotopes.

Chapter 3

Method for locating resonances

3.1 Schrödinger equation

Having constructed the effective η-nucleus potential (folding potential $V_{\eta A}$), we reduced the few-body problem to an effective two-body problem with the Hamiltonian

$$H = -\frac{\hbar^2}{2\mu_s}\Delta_{\vec{r}} + V_{\eta A} \ ,$$

where

$$\mu_s = \frac{m_\eta m_s}{m_\eta + m_s}$$

is the reduced mass for $s = d, t, \tau, \alpha$. The corresponding Schrödinger equation

$$H\Psi = E\Psi \ ,$$

after the partial wave decomposition, takes the form

$$\left[\partial_r^2 + k^2 - \ell(\ell+1)/r^2\right]\psi_\ell(k,r) = U_{\eta A}(r)\psi_\ell(k,r) \ , \tag{3.1}$$

where

$$U_{\eta A}(r) = \frac{2\mu_s}{\hbar^2}V_{\eta A}(r) \tag{3.2}$$

and $k = \sqrt{2\mu_s E/\hbar^2}$ is the η-nucleus relative momentum.

In the calculations, we used the following masses of the particles and reduced masses [26, 20]:

Meson (η):	$m_\eta = 547.45$ MeV,	
Deuteron (d):	$m_d = 1876.136$ MeV,	$\mu_d = 423.789646$ MeV,
Triton (t):	$m_t = 2809.450$ MeV,	$\mu_t = 458.170754$ MeV,
Helion (τ):	$m_\tau = 2809.431$ MeV,	$\mu_\tau = 458.170248$ MeV,
Helium (α):	$m_\alpha = 3728.425$ MeV,	$\mu_\alpha = 477.358732$ MeV.

3.2 First order equations

Following Ref. [22, 27, 28, 29], we look for solution of Eq. (3.1) in the form

$$\psi_\ell(k,r) = h_\ell^{(-)}(kr)F_\ell^{(\mathrm{in})}(k,r) + h_\ell^{(+)}(kr)F_\ell^{(\mathrm{out})}(k,r) \ , \tag{3.3}$$

where the incoming and outgoing waves $h_\ell^{(-)}(kr)$ and $h_\ell^{(+)}(kr)$ are embedded explicitly, and two new unknown functions $F_\ell^{(\mathrm{in})}(k,r)$ and $F_\ell^{(\mathrm{out})}(k,r)$ are introduced. As was shown in Ref. [23], these functions obey the system of coupled first-order equations

$$\left\{\begin{array}{rcl} \dfrac{d}{dr}F_\ell^{(\mathrm{in})} & = & -\dfrac{1}{2ik}h_\ell^{(+)}U_{\eta A}\left[h_\ell^{(-)}F_\ell^{(\mathrm{in})}+h_\ell^{(+)}F_\ell^{(\mathrm{out})}\right] \\ \dfrac{d}{dr}F_\ell^{(\mathrm{out})} & = & \dfrac{1}{2ik}h_\ell^{(-)}U_{\eta A}\left[h_\ell^{(-)}F_\ell^{(\mathrm{in})}+h_\ell^{(+)}F_\ell^{(\mathrm{out})}\right] \end{array}\right. \tag{3.4}$$

with the boundary conditions

$$\lim_{r\to 0} F_\ell^{(\mathrm{in/out})}(k,r) = 1 \ . \tag{3.5}$$

This system is equivalent to the initial Schrödinger equation (3.1) but is more convenient for solving the resonance problem.

3.3 Jost function and spectral points

The differential equations (3.4) can be numerically solved from the origin to a sufficiently far point $r = R$ where the potential vanishes (causing the right-hand sides of the equations to disappear) and therefore $F_\ell^{(\mathrm{in/out})}(k,r)$ become constant. These constants

$$f_\ell^{(\mathrm{in})}(k) = \lim_{r\to\infty} F_\ell^{(\mathrm{in})}(k,r) \tag{3.6}$$

and

$$f_\ell^{(\mathrm{out})}(k) = \lim_{r\to\infty} F_\ell^{(\mathrm{out})}(k,r) \tag{3.7}$$

are the Jost functions that determine asymptotic behavior of the wave function (see, for example, Ref. [30])

$$\psi_\ell(k,r) \underset{r\to\infty}{\longrightarrow} h_\ell^{(-)}(kr)f_\ell^{(\mathrm{in})}(k) + h_\ell^{(+)}(kr)f_\ell^{(\mathrm{out})}(k) \ . \tag{3.8}$$

It is worthwhile to mention that we use here the notation $f_\ell^{(\mathrm{in/out})}(k)$ which is different from the traditional notation such as $f_\ell^{(\pm)}(\pm k)$. There are two reasons for this. First of all, we do not fix the normalization of the solution $\psi_\ell(k,r)$. As a result, both $f_\ell^{(\mathrm{in})}(k)$ and $f_\ell^{(\mathrm{out})}(k)$ can have an arbitrary common factor. We are not concerned with this factor because no observable quantity depends on it. In contrast to a majority of other studies, we leave the normalization of the Jost functions free, and therefore need a notation that is different from the traditional. The second reason is that the superscripts (*in*) and (*out*) are unambiguous and thus we avoid possible confusion caused by the existence of notations with opposite signs for the same Jost functions.

There are certain discrete points in the complex k-plane (bound, resonant, and virtual states), at which the physical wave function (3.3) has only outgoing waves in its asymptotic behavior (3.8). Therefore at these so called *spectral points* we have

$$f_\ell^{(\mathrm{in})}(k) = 0 \ . \tag{3.9}$$

As is seen, the distribution of the spectral points in the complex k-plane (determined by this equation) does not, as was mentioned earlier, depend on the normalization of the Jost function.

3.4 Resonances

Resonance states are formed when quantum particles collide at certain (resonant) energies. Before moving apart, they stay together for a while. During the resonance lifetime, the particles move around each other and "forget" the direction from which they came. Therefore, when the resonance eventually decays, the particles "choose" the direction to move away at random.

In quantum mechanics, this physical concept is mathematically formulated as follows (see, for example, Ref. [30]). Resonant states are spectral points (the above mentioned certain energies), i.e. eigenstates of the Hamiltonian with pure outgoing-wave asymptotics (which means no "memory" of the incoming information).

Therefore, resonances are spectral points, i.e. such points in the complex momentum plane, where the Jost function is zero. The probabilities of possible outcomes of the collision are determined by the S-matrix, which is the ratio of the asymptotic coefficients,

$$S_\ell(k) = \frac{f_\ell^{(\mathrm{out})}(k)}{f_\ell^{(\mathrm{in})}(k)} \ , \tag{3.10}$$

and therefore has poles at all spectral points. A resonance energy,

$$E = E_\mathrm{r} - \frac{i}{2}\Gamma \ , \tag{3.11}$$

has a negative imaginary part, which is called resonance width. The width Γ determines how long the resonance lives. Indeed, the probability of finding the system at any given place,

$$|\Psi(t_0)e^{-iE(t-t_0)}|^2 = |\Psi(t_0)|^2 e^{-\Gamma(t-t_0)} \ ,$$

exponentially diminishes with time due to imaginary part of the energy. Another meaning of Γ is that it defines a window around the collision energy E_r, within which the resonance can be excited.

3.5 Complex rotation

The differential equations (3.4) enable us to obtain a complete solution of the ηA scattering problem at any energy of physical interest. Their advantage over the corresponding Schrödinger equation becomes especially evident when we consider complex values of the energy.

As is shown in Refs. [22, 23], the scheme described in previous sections, enables us to overcome well-known difficulty caused by the divergence of Jost solutions in the resonance domain of the complex momentum plane.

The origin of the difficulty can be understood if we look at the Riccati-Hankel function $h_\ell^{(+)}(kr)$ in the resonance domain of the complex k-plane (below the real axis). As can be seen from its asymptotics

$$h_\ell^{(\pm)}(z) \underset{|z|\to\infty}{\longrightarrow} \mp i \exp\left\{\pm i[z - \ell\pi/2]\right\} \ , \tag{3.12}$$

this function diverges when $r \to \infty$. As a result the right hand side of the first equation of the set (3.4) diverges and hence the limit (3.6) cannot be calculated. It

should be emphasized that this fact does not mean that this limit does not exist. It does exist, but by simply moving along the real r-axis, we cannot reach it. It is easy to see, that

$$\text{if } \ \mathrm{Im}\, kr > 0 \implies h_\ell^{(+)}(kr) \underset{|kr|\to 0}{\longrightarrow} 0 \ . \tag{3.13}$$

When $\mathrm{Im}\, kr = 0$ this function remains finite (oscillates) at large r. The condition $\mathrm{Im}\, kr > 0$ for asymptotic vanishing of the function $h_\ell^{(+)}(kr)$ involves the imaginary part of the product kr but not of the momentum alone. This offers an elegant way to extend the domain of the k-plane where the limit (3.6) can be calculated, to practically whole k-plane. Indeed, if, for example, $\mathrm{Im}\, kr$ is negative we can always make it positive by using complex values of r. This of course requires that the potential is defined for complex r and tends to zero when $|r| \to \infty$ at least in a certain sector of the complex r-plane. In our case, it vanishes when $r \to \infty$ along any line

$$r = z \exp(i\theta) \ , \qquad z \geq 0 \ , \tag{3.14}$$

for the rotation angle θ in the interval $0 \leq |\theta| \leq \theta_{\max} < \pi/2$. The coefficients $f_\ell^{(\mathrm{in/out})}(k)$ in the wave function asymptotics are the same for all choices of the rotation angle because they do not depend on r. By considering complex r, we actually do the analytic continuation of $f_\ell^{(\mathrm{in})}(k)$ to the domain where Eqs. (3.4) do not give finite values for this function.

Chapter 4

Results

The low-energy ηN and η-nucleus interaction is dominated by the S_{11} resonance, which means that all higher partial waves make a negligible contribution as compared to the one coming from the S-wave. In all our calculations, we therefore assume that $\ell = 0$.

In order to locate possible η-nucleus resonances, we searched for zeros of the Jost function $f_\ell^{(\mathrm{in})}(k)$ in the fourth quadrant of the complex k-plane. The search was done using the Newton's method [31]. For each point in the k-plane, the Jost function was obtained by solving the differential equations (3.4) from $r = 0$ to a point sufficiently far from the origin where the potential vanishes and the function $F_\ell^{(\mathrm{in})}(k, r)$ reaches its limit value (3.6). To avoid the divergence, the integration of the differential equations was done along the line (3.14) in the complex r-plane with the rotation angle θ such that $\mathrm{Im}\, kr$ remains positive.

The resonances thus found are given in Tables 4.1-4.4, where the resonance momentum k and the energy

$$E = E_\mathrm{r} - \frac{i}{2}\Gamma$$

are related as

$$E = \frac{k^2}{2\mu_s} \ .$$

The positions of the Jost function zeros (i.e. the S-matrix poles) given in Tables 4.1-4.4, are shown in Figs. 4.1-4.8. For each nuclear system (d, t, τ, and α), these zeros are shown both in the momentum and energy planes. For all isotopes considered, the distribution of the Jost function zeros in the energy plane follows almost vertical line. This means that the resonances completely overlap each other. Since the width Γ increases very fast with the resonance number, only the first resonance for each nucleus may be discern in the scattering or final state interaction picture. All higher resonances form a collective background.

$\mathrm{Re}\, k$ (fm^{-1})	$\mathrm{Im}\, k$ (fm^{-1})	E_r (MeV)	Γ (MeV)
0.516676386	-0.250053354	9.39	23.74
0.557757739	-0.466126622	4.31	47.78
0.850332662	-0.734765811	8.42	114.81
0.749837117	-0.581803575	10.28	80.17
0.944632738	-0.816615407	10.36	141.75
1.051964840	-0.926330329	11.42	179.06
1.126248400	-1.014329900	11.01	209.92
1.234325320	-1.111359490	13.25	252.08

Table 4.1: η-d resonances.

$\mathrm{Re}\, k$ (fm^{-1})	$\mathrm{Im}\, k$ (fm^{-1})	E_r (MeV)	Γ (MeV)
0.909378894	-0.219888233	33.09	33.99
1.081057020	-0.603766038	34.17	110.94
1.237657840	-0.927171221	28.56	195.04
1.348924640	-1.079850840	27.77	247.58

Table 4.2: η-t resonances.

$\mathrm{Re}\, k$ (fm^{-1})	$\mathrm{Im}\, k$ (fm^{-1})	E_r (MeV)	Γ (MeV)
0.891738122	-0.226294155	31.61	34.30
1.059055894	-0.604922991	32.11	108.90
1.213812711	-0.917415813	26.84	189.28
1.330761160	-1.066909850	26.88	241.32

Table 4.3: $\eta - \tau$ resonances.

$\mathrm{Re}\, k$ (fm^{-1})	$\mathrm{Im}\, k$ (fm^{-1})	E_r (MeV)	Γ (MeV)
1.23264042	-0.198489492	60.36	39.92
1.40505908	-0.571114105	67.21	130.92
1.58269994	-0.951647370	65.23	245.72

Table 4.4: $\eta - \alpha$ resonances.

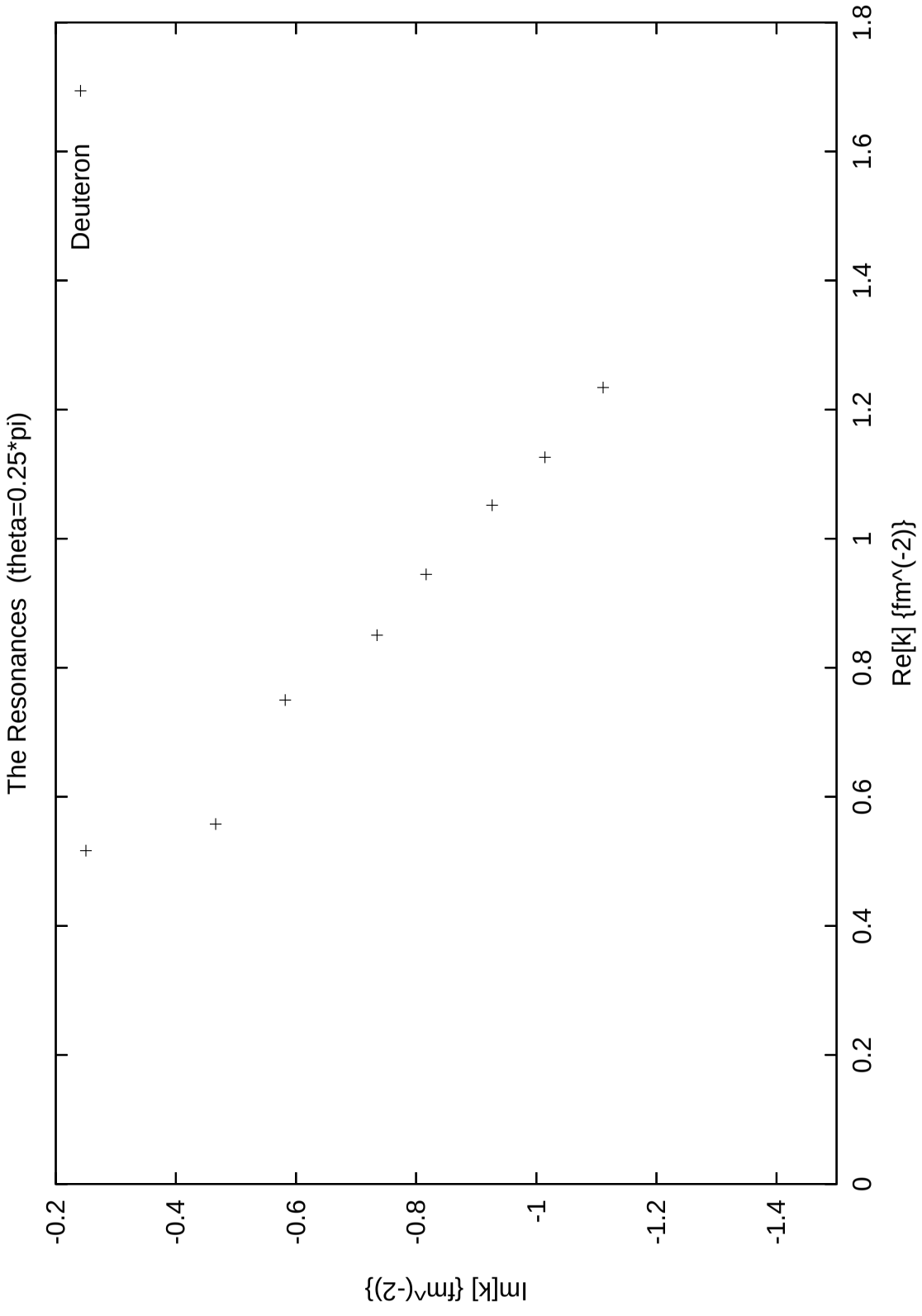

Figure 4.1: Zeros of the η-d Jost function in the k-plane.

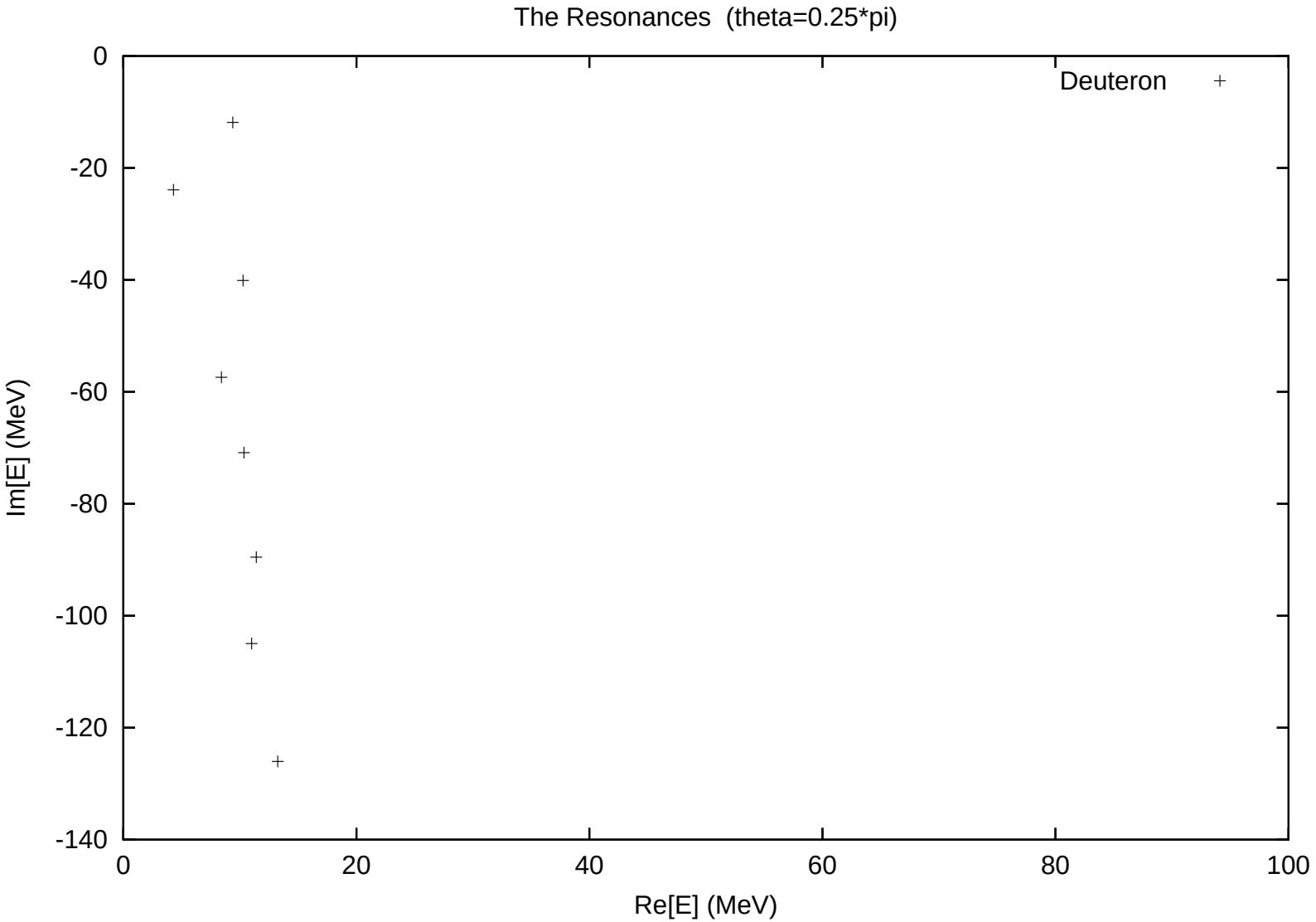

Figure 4.2: Zeros of the η-d Jost function in the E-plane.

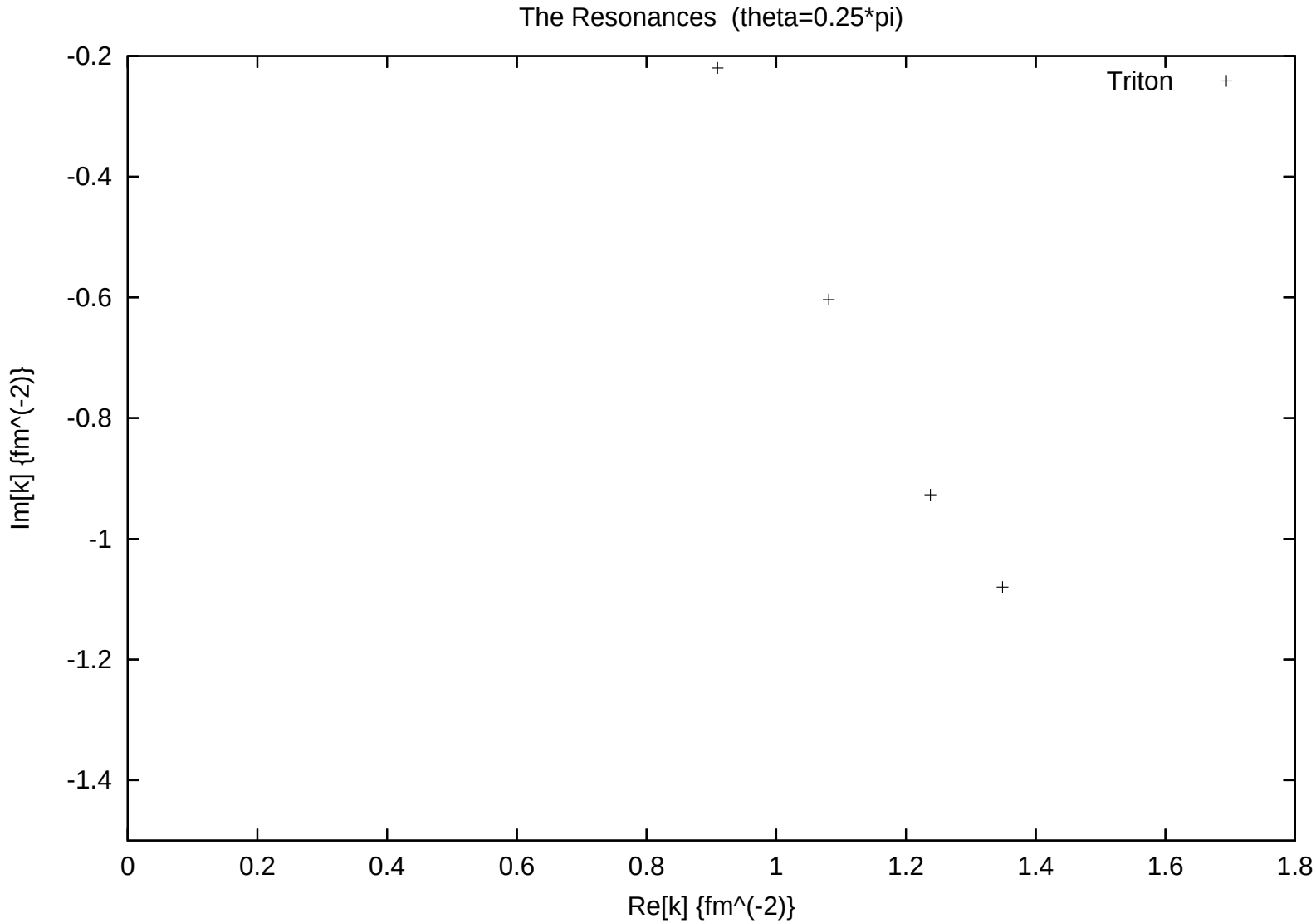

Figure 4.3: Zeros of the η-t Jost function in the k-plane.

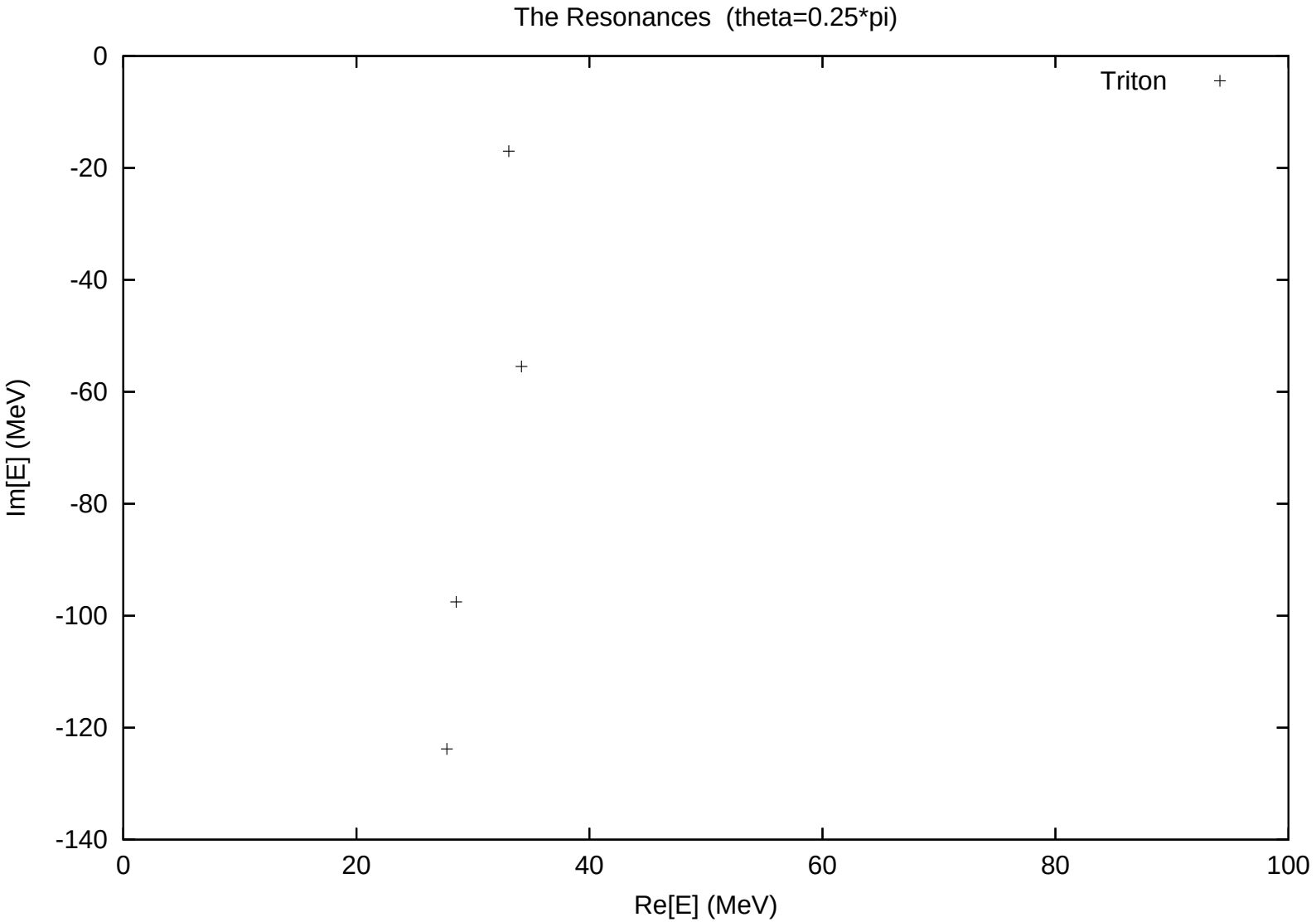

Figure 4.4: Zeros of the η-t Jost function in the E-plane.

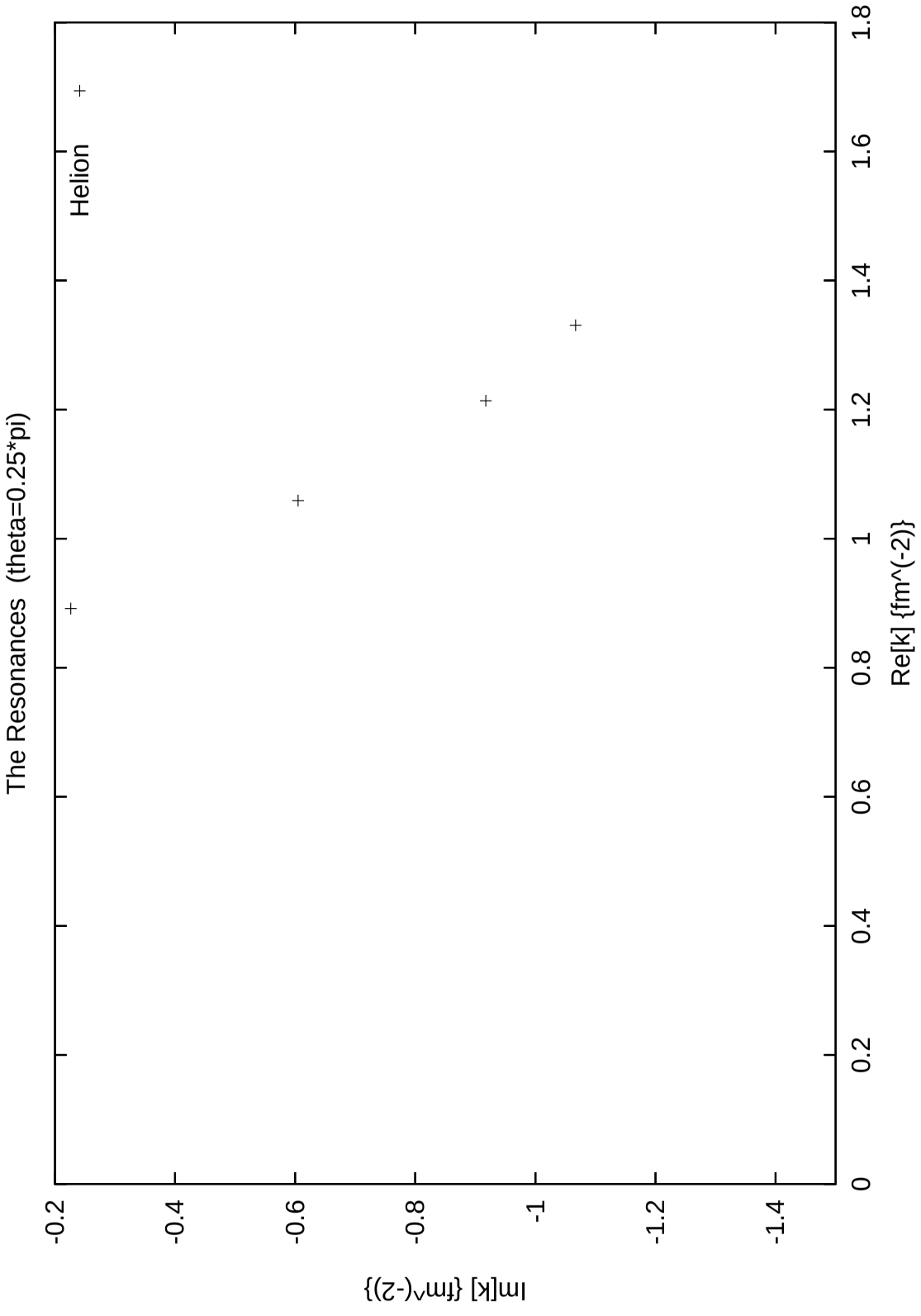

Figure 4.5: Zeros of the η-τ Jost function in the k-plane.

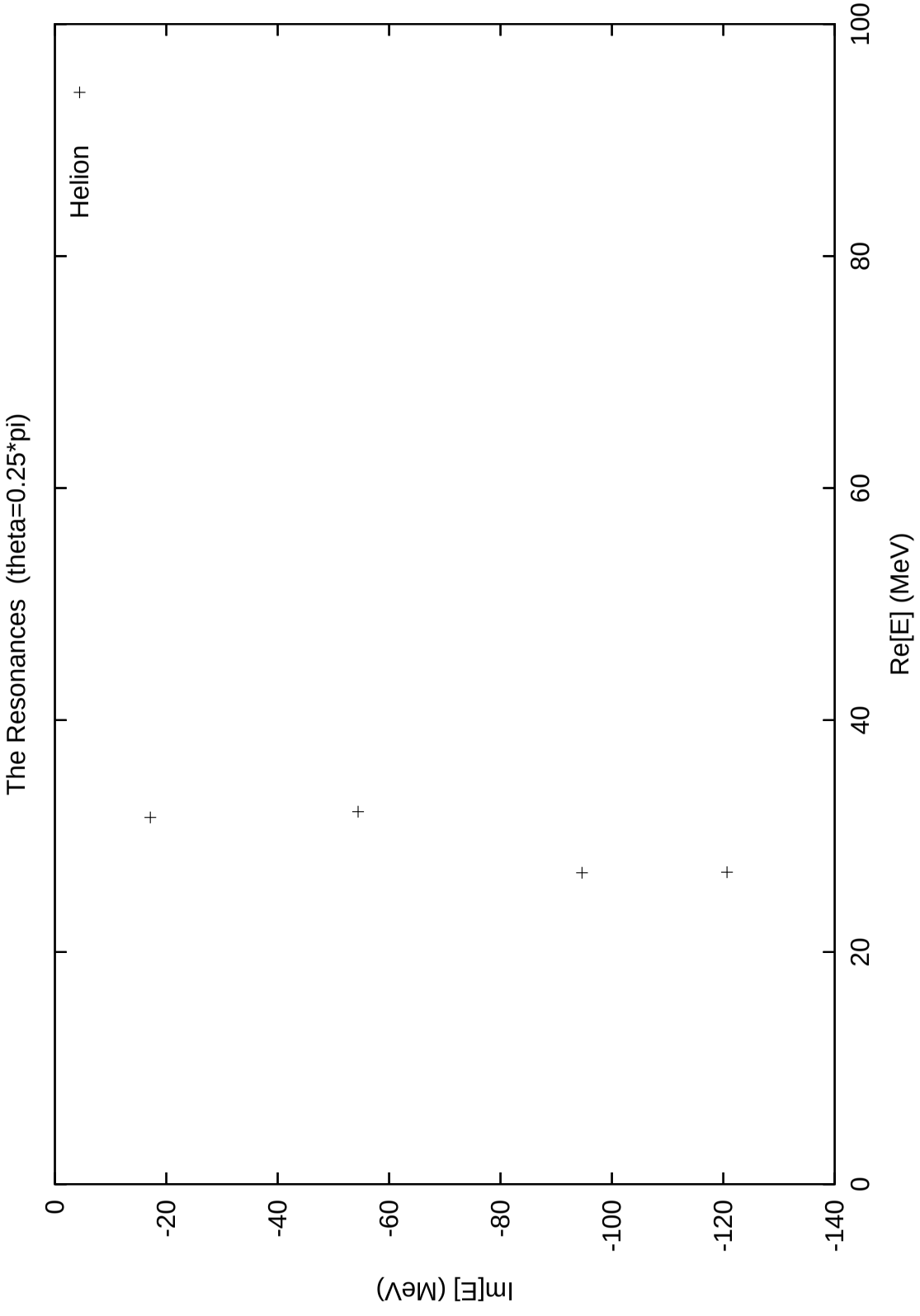

Figure 4.6: Zeros of the η-τ Jost function in the E-plane.

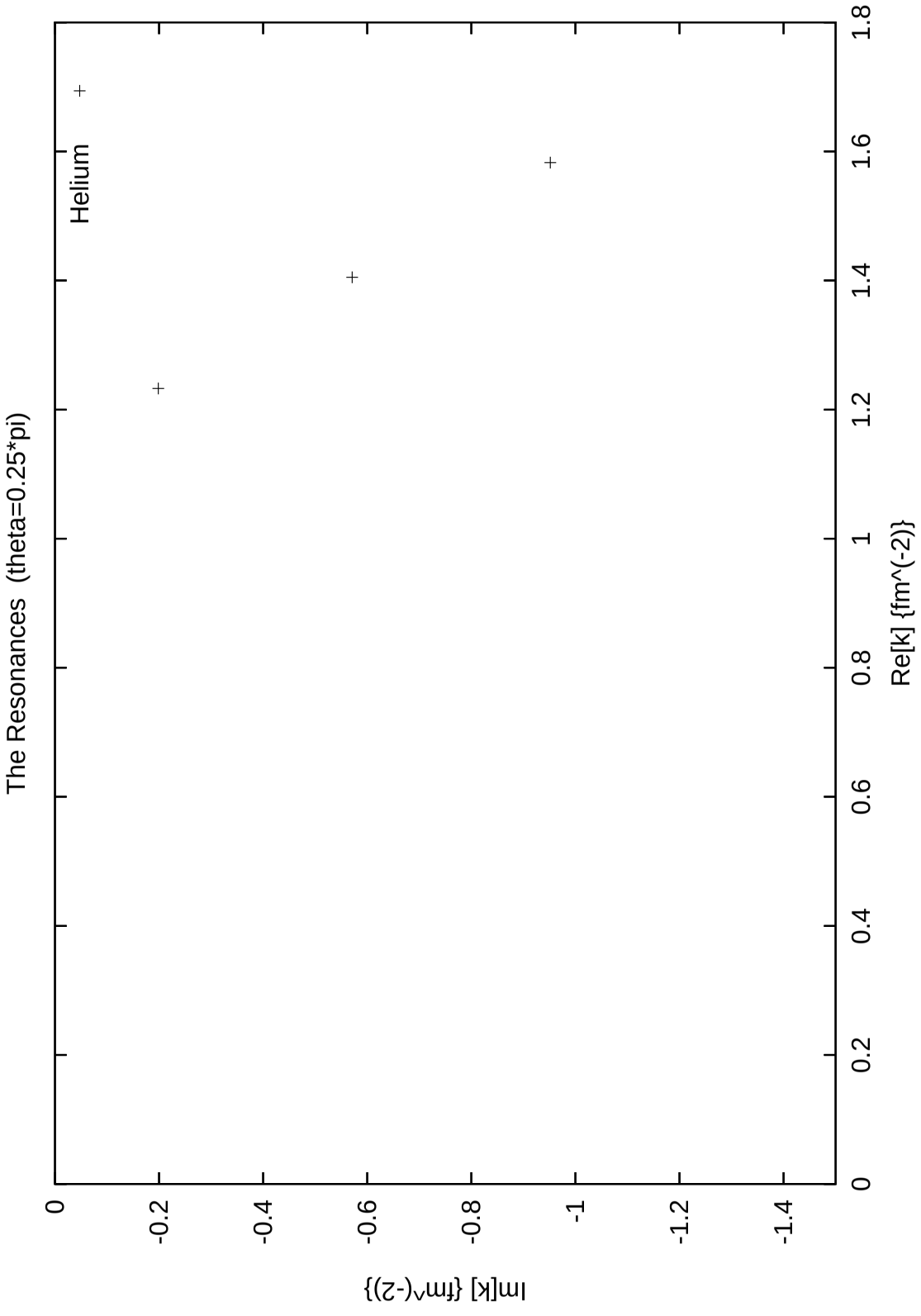

Figure 4.7: Zeros of the η-α Jost function in the k-plane.

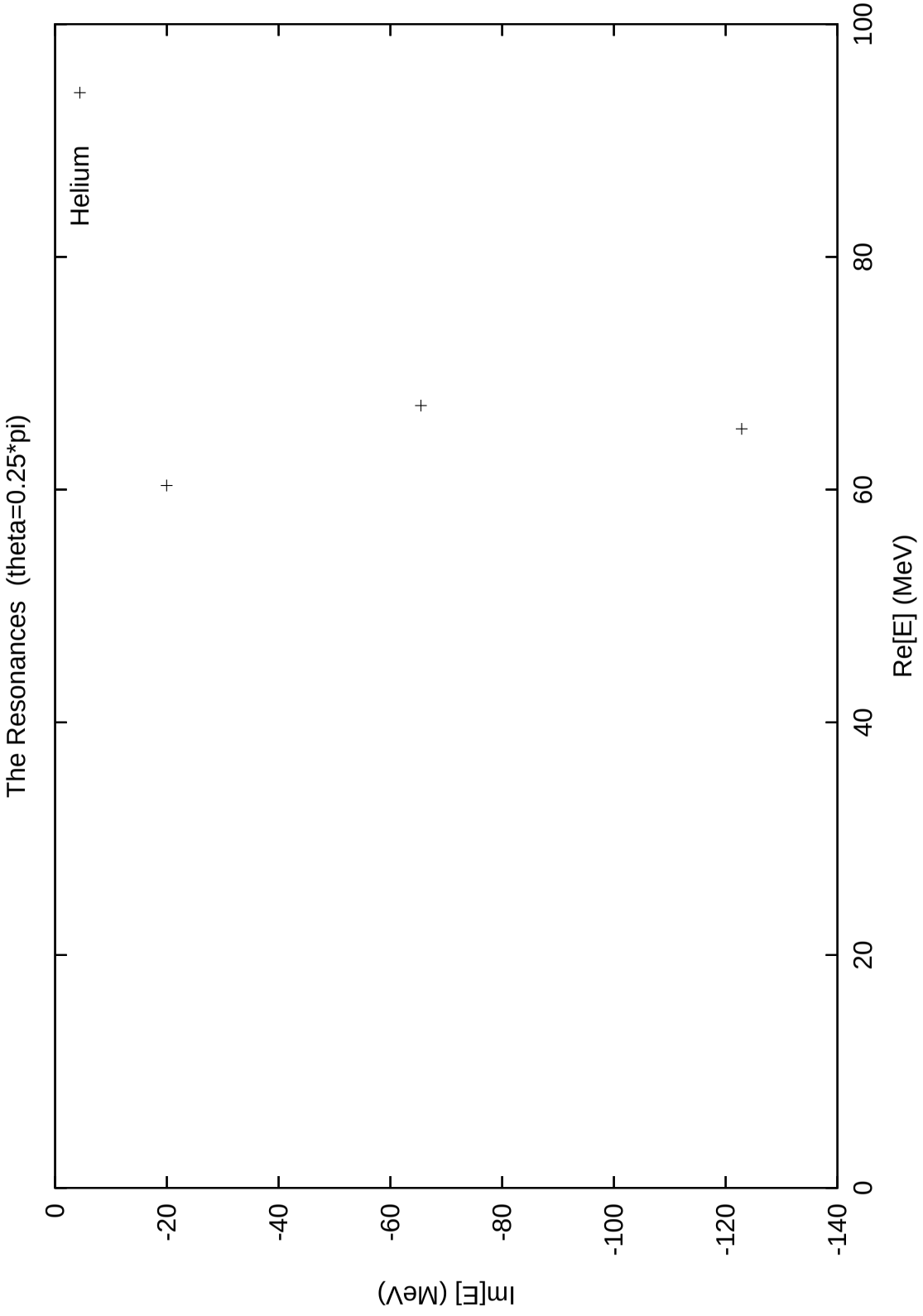

Figure 4.8: Zeros of the η-α Jost function in the E-plane.

Chapter 5

Conclusions

This investigation was devoted to the search of possible resonance states of the systems consisting of the η-meson and the isotopes of hydrogen and helium. To do the search, we first constructed a local ηN potential by fitting the S_{11} resonance and the ηN scattering length. Then, for each of the four isotopes, an η-nucleus potential was constructed within the folding model. This folding potential was used within the Jost function method. Solving the linear first-order differential equations of this method, from the origin to a sufficiently far point along a complex-rotated coordinate, we were able to calculate the Jost function in the fourth quadrant of the complex momentum plane. According to the rigorous definition of quantum resonances, the zeros of this function in the fourth quadrant of the k-plane are the resonances we were looking for.

The results of our calculations show that all considered isotopes support strings of completely overlapping resonances. The widths of the resonances belonging to each string grows very fast with the resonance number. This means that the first resonance of a string may manifest itself on the background formed by all higher resonances.

The resonances for the t and τ systems are very close to each other. This is due to the fact that the number of nucleons in these nuclei are the same. The only difference between them comes from a slight variation in the mean square radius. This radius determines the density distributon spread. The mass difference makes a negligible effect.

When comparing with the other nuclei, i.e. with deuteron (d) and ^{4}He (α), nucleon number difference is important. This is due both to the multiplicities of contribution each nucleon makes to the density in the nuclei, and the specific differences in the density distributions.

No quasibound state has yet been discovered in any experiment [21]. Meanwhile, there are many different predictions based on scattering length calculations, which however have serious drawbacks and therefore are inadequate [18]. The results obtained in this dissertation, are based on a rigorous Jost function method and therefore are more reliable. Of course our predictions cannot be considered as exact and final because they were obtained with an ηN potential constructed using limited experimental data. A more precise potential would slightly shift the resonance positions, but the general picture would remain intact.

Bibliography

[1] Pevsner A., Kraemer R., Nussbaum M., Richardson C., Schlein P., Strand R., Toohig T., Block M., Engler A., Gessaroli R., and Meltzer C. (1961). Evidence for a Three-Pion Resonance Near 550 MeV. Phys. Rev. Lett. **7** 421-423.

[2] Dover C. B. and Fishbane P. M. (1990). η and η' scattering: A probe of the strange-quark ($s\bar{s}$) content of the nucleon. Phys. Rev. Lett. **64** 3115-3118.

[3] Nefkens B. M. K. (1995). Few-Body Systems Suppl. **9** 193.

[4] Montanet L. et al. (Particle Data Group) (1994). Review of Particle Properties. Phys. Rev. **50** 1173-1814.

[5] Coon S. A. and Scadron M. D. (1982). Role of $\pi^0\eta'$ mixing in nuclear charge asymmetry. Phys. Rev. **C26** 562-569.

[6] Wilkin C. (1994). Charge symmetry breaking in the $dd \to \alpha\pi^0$ reaction. Phys. Lett. **B331** 276-279.

[7] Magiera A. and Machner H. (2000). Charge and isospin symmetry breaking via external $\pi^0 - \eta$ meson mixing. Nucl. Phys. **A674** 515-523.

[8] Ceci S., Hrupec D. and Svarc A. (1999). The importance of the nucleon-nucleon correlations for the $\eta\alpha$ S-wave scattering length, and the π^0-η mixing angle in the low-energy $\eta\alpha$ scattering length model. J. Phys. **G25** L35-L41.

[9] Bhalerao R. S. and Liu L. C. (1985). Off-shell model for threshold pionic eta production on a nucleon and for eta-N scattering. Phys. Rev. Lett. **54** 865-868.

[10] Haider Q. and Liu L. C. (1986). Formation of an eta-mesic nucleus. Phys. Lett. **172B** 257-260.

[11] L.C. Liu, Q. Haider. Signature of the Existence of η-Mesic Nucleus. Physical Review **C34** (1986) p1845.

[12] Chrien R. E., Bart S., Pile P., Sutter R., Tsoupas N., Funsten H. O., Finn J. M., Lyndon C., Punjabi V., Perdrisat C. F., Lieb B. J., Kishimoto T., Liu L. C., Estep R., Dropesky B., Stronach C. E., and Stearns R. L. (1988). Search for Bound States of the eta Meson in Light Nuclei. Phys. Rev. Lett. **60** 2595-2598.

[13] Wilkin C. (1993). Near-threshold production of eta mesons. Phys. Rev. **C47**, R938-R940.

[14] Hoffmann-Rothe P., Krebeck M., Hey J., Breuer M., Edel G. V., Hourany E., Rigney M., Ajaka J., Anton G., Arends J., Berrier-Ronsin G., Beulertz W., Blanpied G., Bock A., Didelez J.-P., Helbing K., Maass R., Neldeke G., Preedom B., Richie B., Rosier L., Saghai B., Schumacher M., and Smend F. (1997). Break-up and Coherent Photoproduction of eta Mesons on the Deuteron. Phys. Rev. Lett. **78** 4697-4700.

[15] Calén H. et al. (1998). Threshold Structure of the Quasifree $p + n \rightarrow d + \eta$ Reaction. Phys. Rev. Lett. **80** 2069-2072.

[16] Rakityansky S. A., Sofianos S. A., Sandhas W. and Belyaev V. B. (1995). Threshold scattering of the η-meson off light nuclei. Phys. Lett. **B359** 33-38.

[17] Rakityansky S. A., Sofianos S. A., M. Braun, Sandhas W., and Belyaev V. B. (1996). Quasi-bound states of η-nucleus systems. Phys. Rev. **C53** R2043-R2047.

[18] Svarc A., Ceci S. (2000). η Production in Hadronic Interaction. http://ArXiv.org/abs/nucl-th/0009024.

[19] Krusche B. (2005). Photoproduction of mesons from nuclei – in-medium properties of hadrons. Progress in Particle and Nuclear Physics **55** 46-70.

[20] P.E. Hodgson, E. Gadioli, E. Gadioli Erba. Introductory Nuclear Physics. Oxford University Press (1997).

[21] Haider Q., Liu L. C. (2002). Dependence of calculated binding energies and widths of η-mesic nuclei on treatment of subthreshold η-nucleon interaction. Phys. Rev. **C66** 045208-1-10.

[22] Sofianos S. A. and Rakityansky S. A. (1997). Exact method for locating potential resonances and Regge trajectories. J. Phys. A: Math. Gen. **30** 3725-3737.

[23] Rakityansky S. A., Sofianos S. A. and Amos K. (1996). A method for calculating the Jost function for analytic potentials. Nuovo Cim. B **111** 363-378.

[24] P.E. Hodgson. Optical Model Potential and Nuclear Density Distributions. Lecture Notes in Physics: Nuclear Optical Model Potential **55** (1976) p88.

[25] I.S. Gradshteyn, I.M. Ryzhik. Table of Integrals, Series, and Products (4th ed.). Academic Press (1965) p337.

[26] W.S.C. Williams (1991). Nuclear and Particle Physics. Oxford University Press.

[27] Rakityansky S. A. and Sofianos S. A. (1998). Jost function for coupled partial waves. J. Phys. A: Math. Gen. **31** 5149-5175.

[28] Sofianos S. A., Rakityansky S. A. and Massen S. E. (1999). Jost function for singular potentials. Phys. Rev. A **60**, 337-343.

[29] Rakityansky S. A. and Sofianos S. A. (1999). Jost function for coupled channels. Few-Body Systems Suppl. **10**, 93-96.

[30] J.R. Taylor (1972). Scattering theory. John Wiley, New York.

[31] Gerald C. F., Wheatley P. O. (1994). Applied Numerical Analysis, (5th ed.). Addison-Wesley, New York, pp. 39-43.